

**NASA TECHNICAL  
MEMORANDUM**

**NASA TM X-74001**

**NASA TM X-74001**

**STRUCTURAL STIFFNESS, STRENGTH AND DYNAMIC CHARACTERISTICS  
OF LARGE TETRAHEDRAL SPACE TRUSS STRUCTURES**

By

Martin M. Mikulas, Jr.

Harold G. Bush

and

Michael F. Card

March 1977



(NASA-TM-X-74001) STRUCTURAL STIFFNESS,  
STRENGTH AND DYNAMIC CHARACTERISTICS OF  
LARGE TETRAHEDRAL SPACE TRUSS STRUCTURES  
(NASA) 50 P HC AC3/MF A01

CSCI 13M

Unclass  
GJ/39 21614

This informal documentation medium is used to provide accelerated or special release of technical information to selected users. The contents may not meet NASA formal editing and publication standards, may be revised, or may be incorporated in another publication.

**NASA**

National Aeronautics and  
Space Administration

Langley Research Center  
Hampton, Virginia 23665

STRUCTURAL STIFFNESS, STRENGTH AND DYNAMIC CHARACTERISTICS  
OF LARGE TETRAHEDRAL SPACE TRUSS STRUCTURES

by

Martin M. Mikulas, Jr., Harold G. Bush, and Michael F. Card  
Langley Research Center

CONTENTS

INTRODUCTION

SYMBOLS

TETRAHEDRAL TRUSS ANALYSIS

Truss Description

Number of Columns In a Tetrahedral Truss

Number of Cluster Joints in a Tetrahedral Truss

Truss Mass

Truss Stiffnesses

Basic Assumptions

Cover Extensional Stiffness

Truss Bending Stiffness

Summary of Equations

Cover Internal Loads

Cover Compressive Strength

SOLUTIONS AND DISCUSSION

Tetrahedral Truss Natural Frequencies

Square Planform Bending Frequency

Beam Bending Frequency

Truss Mass Required to Carry a Given Compressive Load

Truss Mass Required to Carry an Applied Moment

Lateral Deflections Due to a Moment Loading

Lateral Deflections Due to Thermal Distortions

Gravity Gradient Loads

Orbital Transfer Loads

CONCLUDING REMARKS

REFERENCES

APPENDIX A - MASS OF INDIVIDUAL COLUMNS

Aluminum Columns

Buckling Critical Columns

Minimum Gage Thickness Constrained Columns

Results and Discussion

Graphite/Epoxy Columns

Results and Discussion

1. Report No. NASA TM X-74001		2. Government Accession No.		3. Recipient's Catalog No.	
4. Title and Subtitle STRUCTURAL STIFFNESS, STRENGTH AND DYNAMIC CHARACTERISTICS OF LARGE TETRAHEDRAL SPACE TRUSS STRUCTURES				5. Report Date MARCH 1977	
				6. Performing Organization Code 27.620	
7. Author(s) Martin M. Mikulas, Jr.; Harold G. Bush and Michael F. Card				8. Performing Organization Report No.	
9. Performing Organization Name and Address NASA Langley Research Center Hampton, Va. 23665				10. Work Unit No.	
				11. Contract or Grant No.	
12. Sponsoring Agency Name and Address National Aeronautics and Space Administration Washington, D. C. 20546				13. Type of Report and Period Covered Technical Memorandum	
				14. Sponsoring Agency Code	
15. Supplementary Notes					
16. Abstract Physical characteristics of large skeletal frameworks for space applications are investigated by analyzing one concept: the tetrahedral truss, which is idealized as a sandwich plate with isotropic faces. Appropriate analytical relations are presented in terms of the truss column element properties which for calculations were taken as slender graphite/epoxy tubes. Column loads, resulting from gravity gradient control and orbital transfer, are found to be small for the class structure investigated. Fundamental frequencies of large truss structures are shown to be an order of magnitude lower than large earth based structures. Permissible loads are shown to result in small lateral deflections of the truss due to low-strain at Euler buckling of the slender graphite/epoxy truss column elements. Lateral thermal deflections are found to be a fraction of the truss depth using graphite/epoxy columns.					
17. Key Words (Suggested by Author(s)) large space structures, tetrahedral truss, graphite/epoxy, columns			18. Distribution Statement Unclassified - Unlimited		
19. Security Classif. (of this report)		20. Security Classif. (of this page)		21. No. of Pages 50	22. Price* \$4.00

STRUCTURAL STIFFNESS, STRENGTH AND DYNAMIC CHARACTERISTICS  
OF LARGE TETRAHEDRAL SPACE TRUSS STRUCTURES

By

Martin M. Mikulas, Jr., Harold G. Bush, and Michael F. Card  
Langley Research Center

INTRODUCTION

Very large, low mass structures are expected to play an important role in many of NASA's future space missions. These missions include activities such as communications, solar power collection, and earth resource surveillance. The results of a study on possible future space activities are presented in reference 1 and a survey of expected requirements of large space structures is presented in reference 2.

Although specific missions are yet to be defined it is obvious that some form of large open truss structures will be a strong candidate for providing a stiff skeletal reference frame upon which on-orbit functions can be conducted. Considerable research and engineering has gone into truss structures for earth based use (see ref. 3), but very little of the technology is applicable to structures for space use because of mass and transportation restrictions. In reference 4 a concept is presented for obtaining high packaging densities for transportation.

To obtain some insight into the general structural characteristics of very large, low mass truss structures, the tetrahedral truss configuration defined in figures 1 and 2 was chosen as an initial study model. Although other truss geometries could be more efficient for achieving specific application requirements, the tetrahedral truss having pseudo-isotropic elastic properties and being constructed of all identical column members is an excellent configuration for preliminary studies.

In the present paper, simple linear plate-theory-type expressions are derived for the tetrahedral truss where the individual members are "smeared out" or averaged over the surface such that the truss structure is assumed to

behave as an equivalent continuum. These simple expressions are then used to explore the behavior of very large truss structures subjected to loadings anticipated in on-orbit operations. Mass expressions are derived for both aluminum and graphite/epoxy tubular columns and these expressions are in turn used to obtain mass relations for the tetrahedral truss.

## SYMBOLS

a	Column spacing
A	Total planform area of truss
B	Truss width
$A_c$	Column cross sectional area
$C, C_1$	Buckling coefficients
D	Plate flexural bending stiffness
E	Young's modulus
f	Frequency
$g_\xi$	A constant defined by Newton's second law (force = $\frac{\text{mass} \times \text{acceleration}}{g_\xi}$ )
H	Truss depth
h	Lamina thickness
I	Moment of inertia
$\rho$	Column length
L	Truss length
M	Applied moment
$N_c$	Number of columns in a truss
P	Axial load in column
$N_j$	Number of cluster joints in a truss structure
$N_x, N_y, N_{xy}$	Inplane stress resultants
r	Column radius
R	Radius of curvature
$t_e$	Effective thickness

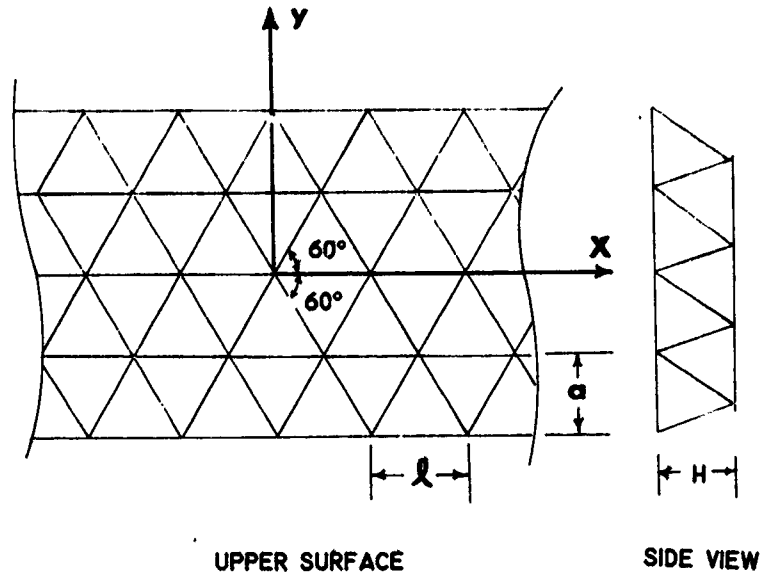
T	Thrust
W	Truss mass
$W_c$	Column mass
x,y	Rectangular coordinates
$\rho$	Mass per unit volume
$\epsilon$	Strain
$\nu$	Poisson's ratio
$\theta$	Column angle defined in Sketch b
$\Delta$	Truss lateral deflection
$\sigma$	Stress
$\eta$	Thrust-to-mass ratio

### TETRAHEDRAL TRUSS ANALYSIS

#### Truss Description

The tetrahedral truss structure considered in this paper is formed with columns lying along the intersections of the sides of repeating tetrahedrons connected at their bases as shown in figure 1-a and connected with additional columns at their upper vertices as shown by the dashed lines in figure 1-b. This arrangement forms an upper and lower cover of triangular column networks separated by a tetrahedron shaped core. A basic repeating element of this structure is shown in figure 1-c where each of the 6 core members are visualized as being split along their length into 1/2 columns. For each repeating element there are 3 columns in the lower cover, 3 columns in the upper cover, and half of 6 columns in the core for a total of 9 columns per repeating element. A photograph of a typical tetrahedron and the resulting tetrahedral truss structure is shown in figure 2. A view of the upper surface of the truss and

of one side is shown in sketch a.



Sketch a.- Tetrahedral truss dimensions  
and coordinate system

The upper surface, which is the same as the lower surface, is a network of columns of length  $l$  forming equilateral triangles. The depth of the structure  $H$  is related to column length  $l$  by

$$H = \sqrt{\frac{2}{3}} l \quad (1)$$

and for future reference the height of each triangle  $a$  is related to column length  $l$  by

$$a = \frac{\sqrt{3}}{2} l$$

### Number of Columns In a Tetrahedral Truss

In evaluating various construction details of a tetrahedral truss structure it is necessary to determine the number of columns required to construct a given size structure. As can be seen in figure 1-c there are effectively 9 columns per repeating element. The projected planform area of each repeating element is  $\lambda a$  so that the number of columns  $N_c$  per unit area is

$$\frac{N_c}{A} = \frac{9}{\lambda a} = \frac{6\sqrt{3}}{\lambda^2} \quad (2)$$

where  $A$  is the total planform area of the truss. A log-log plot of  $\frac{N_c}{A}$  as a function of column length,  $\lambda$ , is shown in figure 3.

### Number of Cluster Joints in a Tetrahedral Truss

Another related item of interest in evaluating the tetrahedral truss is the number of cluster joints per unit area required. It is seen in figure 1-c that there are 9 columns per repeating element. Each cluster joint, however, that connects the columns has 9 attachment points, so that there are 2 cluster joints per repeating element on the average. Thus the number of joints  $N_j$  per unit area of truss is

$$\frac{N_j}{A} = \frac{4}{\sqrt{3} \lambda^2}$$

or there are 2/9 as many cluster joints in a tetrahedral truss as there are individual columns.

### Truss Mass

The mass of the basic repeating element shown in figure 1-c is

$$W_{\text{rep. elem.}} = 9W_c = 9\lambda A_c \rho_c \quad (3)$$

where  $W_c$  is the mass of each column,  $A_c$  is the cross-sectional area of each column and  $\rho_c$  is the density of the column material. The area of the repeating element is  $2a$  so the mass per unit area for the complete truss which is the same as the mass per unit area for the repeating element is

$$\frac{W}{A}_{\text{Truss}} = 9 \frac{A_c \rho_c}{a} = 6\sqrt{3} \frac{A_c \rho_c}{l} \quad (4)$$

### Truss Stiffnesses

Basic Assumptions.- In the present paper the tetrahedral truss is considered to be composed of many repeating elements, and it is assumed that the truss stiffness properties may be averaged over its surface. All columns making up the truss are assumed to be pinned so that no local bending of elements occurs. The upper and lower covers of the truss are  $0^\circ, \pm 60^\circ$  arrangements of columns. With the assumption of averaged stiffness properties over the surface, the covers have an isotropic elastic behavior. The transverse shearing flexibility of the tetrahedron shaped core is neglected so that the truss is idealized as a sandwich plate with isotropic face sheets and a rigid core.

Cover Extensional Stiffness.- The extensional stiffness of the ( $0^\circ, \pm 60^\circ$ ) array of columns of the covers as shown in sketch a can be found by using standard laminate theory where each of the three directions of columns is considered as one lamina. The constitutive relations for a laminate are taken from reference 5 as

$$\begin{bmatrix} N_x \\ N_y \\ N_{xy} \end{bmatrix} = \begin{bmatrix} A_{11} & A_{12} & A_{16} \\ A_{12} & A_{22} & A_{26} \\ A_{16} & A_{26} & A_{66} \end{bmatrix} \begin{bmatrix} \epsilon_x \\ \epsilon_y \\ \gamma_{xy} \end{bmatrix} \quad (5)$$

where

$$A_{ij} = \sum_{k=1}^N (\bar{Q}_{ij})_k (z_k - z_{k-1}) \quad (6)$$

For equal thickness lamina, equations (6) reduce to

$$A_{ij} = \sum_{k=1}^N (\bar{Q}_{ij})_k h \quad (7)$$

where  $h$  is the thickness of each lamina.

For each lamina of the  $(0^\circ, \pm 60^\circ)$  array of columns the lamina orthotropic moduli  $Q_{ij}$  which are defined in equation (2-27) of reference 5 are

$$Q_{11}h = \frac{E_c A_c}{a}, \text{ and all other } Q_{ij} = 0 \quad (8)$$

The laminate moduli of the  $(0^\circ, \pm 60^\circ)$  covers are found by transforming the lamina moduli given by equations (8) using standard stiffness transformation equations (equations (2-3) of ref. 5) and substituting into equations (7). This results in the following constitutive relations for the covers.

$$\begin{bmatrix} N_x \\ N_y \\ N_{xy} \end{bmatrix} = \frac{E_c A_c}{a} \begin{bmatrix} 9/8 & 3/8 & 0 \\ 3/8 & 9/8 & 0 \\ 0 & 0 & 3/8 \end{bmatrix} \begin{bmatrix} \epsilon_x \\ \epsilon_y \\ \gamma_{xy} \end{bmatrix} \quad (9)$$

The stiffnesses in equation (9) are the same as an equivalent isotropic sheet with the following properties.

$$E_e t_e = \frac{E_c A_c}{a}, \text{ and } \nu = 1/3 \quad (10)$$

Where  $E_e$  is the modulus and  $t_e$  is the thickness of the equivalent isotropic sheet.

If it is desirable to separate the modulus  $E_e$  and the thickness  $t_e$  a rational approach would be to take the lamina thickness  $h$  as

$$h = \frac{A_c}{a} \quad (11)$$

This process gives an effective laminate thickness of

$$t_e = 3 \frac{A_c}{a} \quad (12)$$

and an effective laminate modulus of

$$E_e = \frac{E_c}{3} \quad (13)$$

In most analyses the laminate stiffness quantity  $E_e t_e$  can be used so that the abstraction of a separate laminate effective modulus or thickness need not be made.

Truss Bending Stiffness.- The bending stiffness  $D$  of a sandwich plate with thin isotropic face sheets is

$$D = \frac{Et H^2}{2(1-\nu^2)} \quad (14)$$

The effective bending stiffness of the tetrahedral truss is found by substituting the values for face sheet stiffness  $E_e t_e$  and face sheet Poisson's ratio  $\nu$  from equations (10) and the value for truss depth from equation (1) into equation (14) to yield

$$D_{\text{Truss}} = \frac{1}{2} E_c A_c a \quad (15)$$

or in terms of the column length  $\ell$

$$D_{\text{Truss}} = \frac{\sqrt{3}}{4} E_c A_c \ell \quad (16)$$

For a tetrahedral truss structure with one long dimension it may be appropriate to characterize the bending behavior as that of a beam. For that case the bending stiffness per unit width of the truss is

$$\left(\frac{EI}{B}\right)_{\text{Truss}} = \frac{4}{9} E_c A_c a \quad (17)$$

where  $B$  is the total width of the truss. In terms of the column length  $\ell$

$$\left(\frac{EI}{B}\right)_{\text{Truss}} = \frac{2}{3\sqrt{3}} E_c A_c \ell \quad (18)$$

### Summary of Equations

As previously stated the tetrahedral truss is treated herein as a sandwich plate with isotropic face sheets and a rigid core. For convenience the pertinent equations are summarized below both in terms of the column length  $\ell$  and in terms of the column spacing  $a$ .

#### Single Cover Extensional Stiffness

$$(E_e t_e)_{\text{cover}} = \frac{E_c A_c}{a} = \frac{2E_c A_c}{\sqrt{3} \ell}, \nu = 1/3 \quad (19)$$

#### Truss Plate Bending Stiffness

$$D_{\text{Truss}} = \frac{1}{2} E_c A_c a = \frac{\sqrt{3}}{4} E_c A_c \ell \quad (20)$$

#### Truss Beam Bending Stiffness

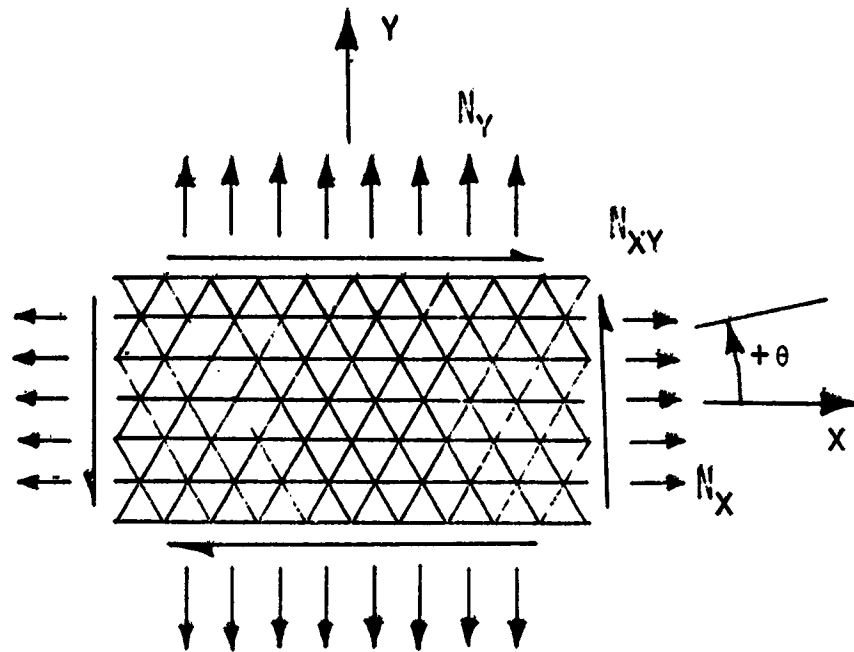
$$\frac{EI}{B}_{\text{Truss}} = \frac{4}{9} E_c A_c a = \frac{2E_c A_c \ell}{3\sqrt{3}} \quad (21)$$

#### Truss Mass Per Unit Area

$$\frac{W}{A}_{\text{Truss}} = 3 \left( \frac{W}{A} \right)_{\text{Covers}} = 9 \frac{A_c \rho_c}{a} = 6\sqrt{3} \frac{A_c \rho_c}{\ell} \quad (22)$$

## Cover Internal Loads

For stress analysis purposes the loadings on the covers are the average resultant loads  $N_x$ ,  $N_y$ , and  $N_{xy}$  as shown in sketch b.



Sketch b.- Average resultant cover loads

In general these running loads are a function of  $x$  and  $y$  and can be related to the individual column loads using standard laminate theory considering the  $(0^\circ, \pm 60^\circ)$  array of columns to behave isotropically. This process results in the following expressions for individual column loads:

$$P_{\pm 60^\circ} = \frac{2}{3} a (N_y \pm \sqrt{3} N_{xy}) \quad (23)$$

and

$$P_{0^\circ} = a (N_x - \frac{1}{3} N_y) \quad (24)$$

where  $a$  is the column spacing. Although the covers behave isotropically from a deformation point of view, equations (23) and (24) show that the loads in the  $\pm 60^\circ$  columns are one third less than the load in the  $0^\circ$  columns for equal  $N_x$  or  $N_y$  loadings. Thus, the direction of highest unidirectional loading on the truss structure should be lined up with the  $y$  axis.

### SOLUTIONS AND DISCUSSION

In this section several simple structural analysis problems are solved on the tetrahedral truss to demonstrate the application of the previously developed analysis. The problems considered are primarily directed towards developing an understanding of the behavior of very large space structures (e.g. planform dimensions on the order of a kilometer or greater).

#### Tetrahedral Truss Natural Frequencies

The first free-free bending frequency of a tetrahedral truss provides a basic insight into the vibrational characteristics of a large truss structure in orbit. The first bending frequency is presented for both a truss structure of square planform and for a truss structure with one long dimensions such that it behaves as a beam.

Square Planform Bending Frequency. - The first bending frequency  $f_p$  for a free-free isotropic square plate is found from reference 6 to be

$$f_p = \frac{14.1}{2\pi L^2} \sqrt{\frac{g_\xi D}{\rho t}} \quad (25)$$

where  $L$  is the length or width of the square plate, and  $\rho t$  is the mass per unit area of the plate and a constant  $g_\xi$  has been introduced to facilitate changes from SI to U.S. customary units. By substituting into equation (25) for the bending stiffness from equation (20) and mass per area from equation (22), the first natural frequency of a tetrahedral truss with square planform is

$$f_p = \frac{14.1}{4\pi\sqrt{6}} \frac{\ell}{L^2} \sqrt{\frac{g_\xi E_c}{\rho_c}} \quad (26)$$

where

$$g_\xi = 1 \frac{\text{kg.m}}{\text{N.sec}^2} \left( 32.2 \frac{\text{lbm.ft}}{\text{lbf.sec}^2} \right)$$

The frequencies as obtained from this equation are plotted in figure 4 as a function of the truss planform dimension  $L$  for several values of column length  $\ell$ . The columns are assumed to be made of graphite/epoxy material. Although the modulus of the unidirectional graphite/epoxy is  $131 \frac{\text{GN}}{\text{m}^2}$  ( $19 \times 10^6$  psi) a nominal value of  $103 \text{GN/m}^2$  ( $15 \times 10^6$  psi) is used to account for the circumferential wraps that are required for increasing local buckling loads and for improving tube handling characteristics.

It may be inferred from figure 4 that very large space structures may have significantly lower frequencies than earth structures. For example, for  $L \sim 300\text{m}$ , large space structures have frequencies of the order of .1 hz (about an order of magnitude lower than conventional earth structures). Although the frequency increases substantially with increasing column length  $\ell$ , considerations such as launch vehicle packing constraints and surface coverings provide practical limitations on the column lengths.

Beam Bending Frequency.- The first bending frequency  $f_b$  for a free-free beam is found from reference 6 to be

$$f_b = \frac{22.37}{2\pi L^2} \sqrt{\frac{g_\xi EI}{\rho A}} \quad (27)$$

where  $L$  is the length of the beam and  $\rho A$  is the mass per unit length of the beam. For a tetrahedral truss structure where  $L$  is the long dimension and  $B$  is the width, equation (27) can be written as

$$f_b = \frac{22.37}{2\pi L^2} \sqrt{\frac{g_\xi EI}{\rho A/B}} \quad (28)$$

where  $\rho A/B$  is the mass per unit area of the truss. By substituting into equation (28) for the bending stiffness from equation (21) and the mass per unit area from equation (22), the first free-free natural frequency of a tetrahedral truss with one long dimension such that it behaves as a beam is

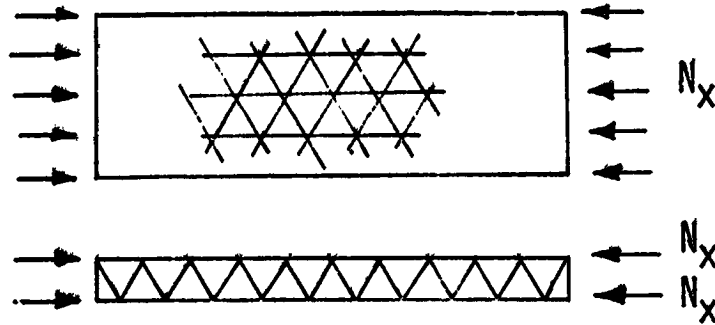
$$f_b = \frac{22.37}{6\pi\sqrt{3}} \frac{\ell}{L^2} \sqrt{\frac{g_\xi E_C}{\rho_C}} \quad (29)$$

To evaluate the accuracy of the present approach an exact calculation of the first natural frequency of a tetrahedral truss 16 bays long and 8 bays wide was made using the NASTRAN finite element computer code. The exact frequency as determined from the NASTRAN calculation was 2% lower than the frequency obtained from equation (29).

#### Truss Mass Required to Carry a Given Compression Load

The tetrahedral trusses treated in the present paper are considered to be made up of identical slender tubular column members. The mass and sizing of the individual members depends, therefore, on the design of the most heavily loaded column. Because of the benign space environment, it is not expected that the columns will be loaded very heavily for space applications so that the critical design condition will be stability of the slender columns due to the compression load in the cover members. The mass strength characteristics of efficient tubular columns are discussed in Appendix A. The loading considered in

this section is a uniform compressive loading  $N_x$  as shown in Sketch c.



Sketch c.- Uniform Compressive Loading on Tetrahedral Truss

For the most critical condition where the  $0^\circ$  columns are in the direction of loading, the load in these individual columns  $P$  is found from equation (24) to be

$$P = aN_x \quad (30)$$

The mass per unit area of a tetrahedral truss is found from equation (22) as

$$\frac{W}{A}_{\text{Truss}} = 6\sqrt{3} \frac{A_{c^0c}}{l} \quad (31)$$

The mass  $W_c$  of an individual column is  $A_c \ell \rho_c$  so that equation (31) can be written as

$$\frac{W}{A}_{\text{Truss}} = 6\sqrt{3} \frac{W_c}{\ell^2} \quad (32)$$

For the assumption that the columns are lightly loaded so that they are designed from material of minimum thickness  $t_m$ , the column mass is obtained from equation (A-9). Substituting into equation (32) yields the following expression for the truss mass in terms of the column load  $P$  . . . . .

$$\frac{W}{A}_{\text{Truss}} = \frac{12\sqrt{3}}{c^{1/3}} \frac{\rho_c}{E^{1/3}} t_m^{2/3} \left(\frac{P}{\ell}\right)^{1/3} \quad (33)$$

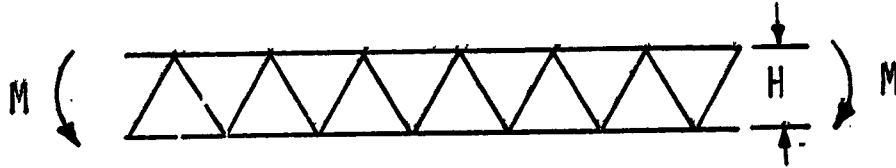
Substituting for  $P$  from equation (30) yields the mass per unit area of a truss in terms of the applied compression load  $N_x$  as

$$\frac{W}{A}_{\text{Truss}} = 12 \left(\frac{9}{2c}\right)^{1/3} \frac{\rho_c}{E^{1/3}} t_m^{2/3} N_x^{1/3} \quad (34)$$

For the minimum gage design condition on the columns, the mass per unit area of a truss is independent of column length.

#### Truss Mass Required to Carry an Applied Moment

The tetrahedral truss treated in this section has an overall length  $L$ , a width  $B$  and is subjected to an applied bending moment  $M$  as shown in Sketch d.



Sketch d.- Tetrahedral truss subjected to an applied moment

The average load per unit length in the covers due to the applied bending moment is

$$N_x = \frac{M}{BH} = \sqrt{\frac{3}{2}} \frac{M}{Bl} \quad (35)$$

The load in the individual columns can be found by substituting for  $N_x$  from equation (30) into equation (35) to obtain

$$P = \frac{3}{2\sqrt{2}} \frac{M}{B} \quad (36)$$

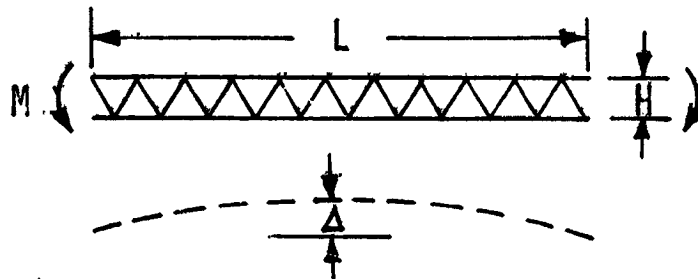
From equation (36), for a tetrahedral truss subjected to an applied moment, the load in the individual columns is independent of the column length. The compression load governs the design, therefore the truss mass per unit area is found by substituting for the column load  $P_c$  from equation (36) into equation (33) to obtain

$$\frac{W}{A}_{\text{Truss}} = \frac{18\sqrt{3/2}}{C^{1/3}} \frac{P_c}{E^{1/3}} t_m^{2/3} \frac{(M/B)^{1/3}}{l^{1/3}} \quad (37)$$

The truss mass per unit area as obtained from equation (37) is plotted in figure 5 as a function of the column length  $\ell$  for different values of the applied moment. Results shown are for graphite/epoxy material and the constants used in equation (37) are the same as those used in Appendix A for the graphite/epoxy columns. For reference the mass per unit area of a 5 mil mylar film and the estimated range of mass per unit area of solar cells (see ref. 2) are also shown in figure 5.

#### Lateral Deflections Due to a Moment Loading

In this section the lateral deflection of a tetrahedral truss subjected to a pure moment is investigated. A schematic of the moment loading  $M$  and the lateral deflection  $\Delta$  are shown in Sketch e.



Sketch e.- Truss loading and resulting deflection

The standard moment curvature relation for a beam is

$$M = EIy'' = EI \frac{1}{R} \quad (38)$$

Considering that  $\sigma = E\epsilon$  and  $\sigma = \frac{MH}{2I}$ , an expression for the upper surface strain in the truss is found from equation (38) as

$$\epsilon = \frac{H}{2R} \quad (39)$$

For small deflections the center deflection  $\Delta$  can be related to the beam length  $L$  and radius of curvature  $R$  by a parabolic expression as

$$\Delta = \frac{L^2}{8R} \quad (40)$$

From equations (39) and (40) an expression for the truss center deflection in terms of the surface strain  $\epsilon$  can be obtained as

$$\Delta = \frac{\epsilon L^2}{4H} \quad (41)$$

In figure 6 the ratio of center deflection  $\Delta$  to the truss depth  $H$  is plotted as a function of the ratio of the truss length  $L$  to the truss depth  $H$  for one value of the strain  $\epsilon$ . The relatively low value of strain was chosen from Appendix A considering that space structures will be very lightly loaded. It can be seen from figure 6 that the deflections of trusses with lengths to depth ratios of a 100 or less are only on the order of the depth of the truss.

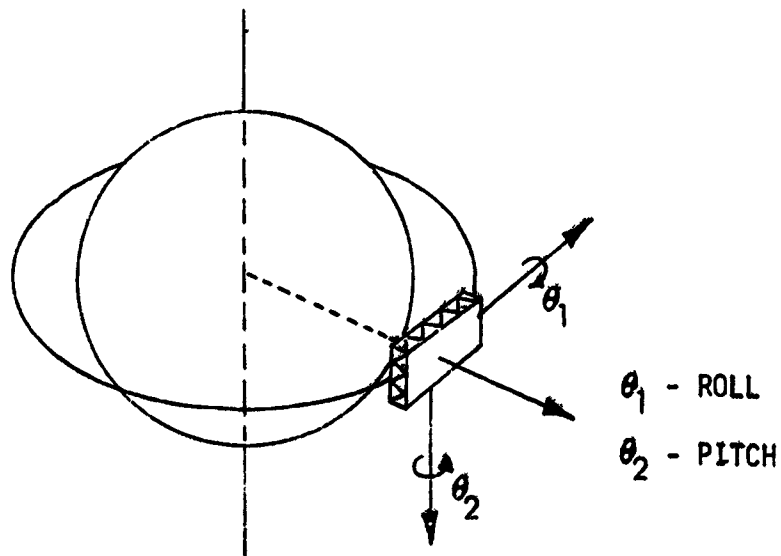
#### Lateral Deflections Due Thermal Distortions

It is likely that one surface of a space structure could get significantly hotter than the other surface due to solar heating. To investigate lateral deflections caused by thermal gradients through the depth of the truss, the analysis of the previous section was extended to include temperature effects. The results of this study are shown on figure 7. The graph is a plot of the ratio of center deflection  $\Delta$  to truss depth  $H$  as a function of the column coefficient of thermal expansion  $\alpha$ . Typical values are shown for the coefficient of thermal expansion of graphite/epoxy, steel, and aluminum. A shaded band is indicated for graphite/epoxy due to the fact that the material could be tailored to achieve different values. The temperature differential between the upper and lower covers of the truss was chosen as 222K (400°F), which is about the maximum that could be expected in an earth orbit. For a

truss structure with a length to depth ratio of 100 it can be seen from figure 7 that an aluminum structure would have center deflections 5 or 6 times the truss depth while a graphite/epoxy structure would have a center deflection less than half of the truss depth.

#### Gravity Gradient Loads

In this section internal loads due to moments which are applied to the structure to counteract gravity gradient effects are investigated. The rotational angles with respect to the orbit are shown in sketch f.



Sketch f.- Orbital angles and structural dimensions

The moments obtained from standard theory on gravity gradients which must be applied to the structure to hold it at a given inclination with respect to the orbit are

$$M_1 = \frac{3k}{2R^3} (I_3 - I_2) \sin 2\theta_1 \cos^2 \theta_2$$

$$M_2 = \frac{3k}{2R^3} (I_3 - I_1) \sin 2\theta_2 \cos \theta_1 \quad (42)$$

and

$$M_3 = \frac{3k}{2R^3} (I_1 - I_2) \sin 2\theta_2 \sin \theta_1$$

where  $R$  is the orbital radius, measured from the center of the earth, and

$$\begin{aligned} k &= g_0 R_e^2 = 3.984 \times 10^{14} \text{ m}^3/\text{sec}^2 \quad (1.407 \times 10^{16} \text{ ft}^3/\text{sec}^2) \\ R_e &= 6373 \text{ km} \quad (3960 \text{ miles}) \\ g_0 &= 9.8 \text{ m/sec}^2 \quad (32.2 \text{ ft/sec}^2) \end{aligned} \quad (43)$$

The moments of inertia of the truss structure are

$$\begin{aligned} I_1 &= \frac{W}{12g_\xi} (B^2 + H^2) \\ I_2 &= \frac{W}{12g_\xi} (L^2 + H^2) \\ I_3 &= \frac{W}{12g_\xi} (L^2 + B^2) \end{aligned} \quad (44)$$

For a truss structure where  $L$  and  $B$  are large compared with  $H$

$$\begin{aligned}
 I_3 - I_2 &\sim \frac{W}{12g_\xi} B^2 \\
 I_3 - I_1 &\sim \frac{W}{12g_\xi} L^2 \\
 I_1 - I_2 &= \frac{W}{12g_\xi} (B^2 - L^2)
 \end{aligned} \tag{45}$$

The maximum restoring bending moment would need to be applied to the structure when  $\theta_2 = 45^\circ$  and  $\theta_1 = 0$ . Using the second of equations (42) and (45) yields this moment as

$$M_2 = \frac{Wk L^2}{g_\xi 8R^3} \tag{46}$$

Using the definition for  $R$  from equation 43 yields

$$M_2 = \frac{Wg_o R_e^2 L^2}{8g_\xi R^3} \tag{47}$$

If it is assumed that this moment is applied as a distributed line moment at the center of the truss, the load in the columns adjacent to the applied moment can be obtained by substituting for the moment from equation (47) into equation (36) to obtain

$$P = \frac{3}{16\sqrt{2}} \frac{Wg_o R_e^2 L^2}{g_\xi B R^3} \quad (48)$$

For the case where all columns in the truss are identical the mass of a truss in terms of the design load  $P_{des}$ , and the column length  $\ell$  can be found from equation (33). Substituting for the truss mass from equation (33) and for the earth radius from equations (43) into equation (48) yields the maximum column load  $P$  due to gravity gradient effects as

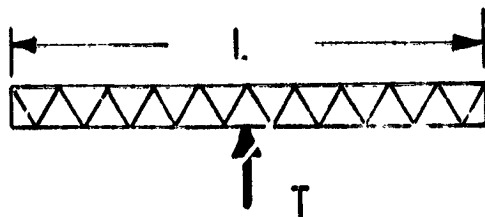
$$P_c = \frac{9}{4} \sqrt{\frac{3}{2}} \left[ \frac{g_o \rho_c t_c^{2/3}}{g_\xi E_c^{1/3}} \right] R_e^2 \left( \frac{L}{R} \right)^3 \left( \frac{P_{des}}{\ell} \right)^{1/3} \quad (49)$$

A plot of the column load as obtained from equation (49) is presented in figure 8 as a function of the truss overall length  $L$  for three values of column length  $\ell$  for the worst case of a low earth orbit (LEO). The truss structures considered in figure 8 all have columns designed to carry a compressive load of a 4448N (1000 pounds). For truss structures with a length of 1.6km or less the resultant column load from the centrally located line moment is small compared with the design load of a 4448N. These calculations consider only the mass of the structure and that surface covering mass if any would have to be added to the total mass considered in equation (48).

#### Orbital Transfer Loads

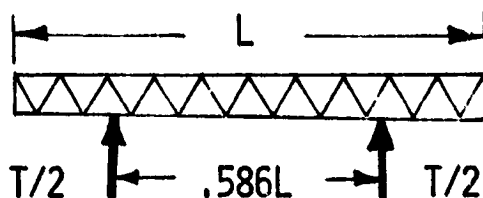
One concept for transferring large space structures from a low earth orbit to geosynchronous orbit is to use very high specific impulse, ion propulsion engines. Although the acceleration resulting from such a propulsion system is typically very low (see ref. 2) the loading developed must be considered because of the fragile nature of very large space structures. To investigate internal loads that may result from this type of propulsion system, three different arrays of engine locations were considered. The first is an array of engines located along the center line of the truss structure as shown

in sketch g.



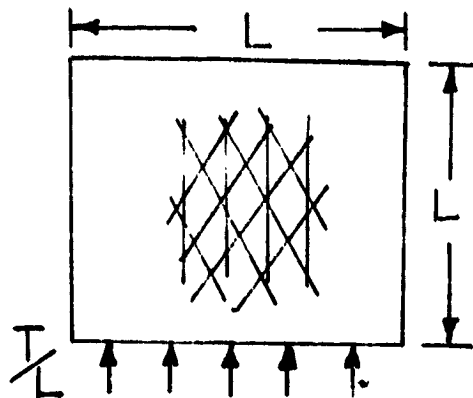
Sketch g.- Centrally located line of ion thrust engines

The thrusting configuration shown in sketch g obviously results in a relatively large bending moment at the center of the structure. To reduce this bending moment a second configuration was studied where two lines of engines were placed such that the bending moment would be a minimum. This configuration is shown in sketch h.



Sketch h.- Dual line of ion thrust engine located to minimize bending moment

The third configuration studied was a line of ion engines placed on the edge of the truss structure so as to produce only inplane loadings. Such a configuration is shown schematically in Sketch i.



Sketch i.- Ion engines placed on the edge of the truss structure

In each of the three previously mentioned propulsion configurations the critical design consideration is the maximum compressive load in cover columns. For the configuration shown in Sketch g the centrally located line thrust produces a bending moment at the center of the truss which results in a lower cover compressive load  $P$  in the columns as follows:

$$P = \frac{3\eta}{16\sqrt{2}} \left[ \left(\frac{W}{A}\right)_{\text{Str.}} + \left(\frac{W}{A}\right)_{\text{Non.Str.}} \right] L^2 \quad (50)$$

where  $\eta$  is the thrust to mass ratio,  $\left(\frac{W}{A}\right)_{\text{Str.}}$  is the mass per unit area of the truss structure and  $\left(\frac{W}{A}\right)_{\text{Non.Str.}}$  is the mass per unit area of the non-structural coverings or equipment which are added. The comparable expression for maximum compressive column load which results from the thrust configuration shown in Sketch h is given by

$$P = .022\eta \left[ \left(\frac{W}{A}\right)_{\text{Str.}} + \left(\frac{W}{A}\right)_{\text{Non Str.}} \right] L^2 \quad (51)$$

while the maximum compressive column load resulting from the thrust configuration given in Sketch i is:

$$P = \frac{\sqrt{3}\eta}{2} \left[ \left(\frac{W}{A}\right)_{\text{Str.}} + \left(\frac{W}{A}\right)_{\text{Non Str.}} \right] L \quad (52)$$

In figure 9 a plot of the maximum compressive column load in a square truss structure is presented as a function of the planform width  $L$  for the three different configurations just discussed. The mass per unit area of the truss structure used in equation (50) was taken from equation (33) for a column design load of 4448N (1000 lbf) and a length of 18.3m (60 ft). The

non-structural mass per unit area was taken as 4 times the structural mass value. The thrust to mass ratio  $\eta$  was taken as 0.0098 Newton/kg ( $.001 \frac{\text{lb}_f}{\text{lb}_m}$ ). This value would result in a transfer time from low earth orbit to geosynchronous orbit of about one week (see ref. 2). Considering these design conditions it can be seen from figure 9 that for the central lateral line load of engines the column design load of 4448N would be exceeded for a structure about 1.6km square. For the double line load the column load is reduced to 17 percent of the single line load value which permits the structure to extend to about 3.2km in extent before the design load is exceeded. For the edge loading configuration the resultant column loads are reduced by an order of magnitude or greater for the parameters considered which essentially eliminates the orbital transfer load as a critical structural design condition.

#### CONCLUDING REMARKS

Simple expressions for the structural stiffness, strength, and dynamic characteristics of a representative tetrahedral large space truss structure are developed and numerically demonstrated. To obtain these expressions properties of individual elements (columns) are averaged over the surface such that the truss structure is assumed to be an equivalent continuum. This approximation results in the truss structure being treated as a sandwich plate with a rigid core. For the structure considered in this paper the truss covers possess a "pseudo-isotropic" behavior which results in very simple expressions for the structural behavior. Although in the present paper attention is restricted to the tetrahedral truss structure with identical individual elements (columns), the approach can be used for most planar truss structures formed from a series of many repeating elements.

To understand the characteristics that very large space might possess, the simple expressions developed in this paper are used to study the behavior of truss structures subjected to conditions anticipated in on-orbit operations. The primary material system considered is graphite/epoxy. The studies include natural vibration frequencies, truss mass required to carry representative

loadings, truss deflections due to mechanical and thermal loadings, and internal loads resulting from gravity gradient and orbital transfer considerations. Observations based on these limited studies indicate the following:

1. The global behavior of the tetrahedral truss structure can be accurately determined using the equivalent continuum approach developed herein.
2. The first natural frequencies of very large space structures can be an order of magnitude lower than earth-based structures.
3. Internal column loads due to anticipated loadings in space are very low.
4. Allowable lateral deflections of very large weight-efficient tetrahedral truss structures are only on the order of the depth of the truss.
5. The large tetrahedral truss structures considered herein have a relatively low mass per unit area (about  $\text{kg/m}^2$  (.05  $\text{lbm/ft}^2$ )).

The analysis procedure developed in this paper provides a simple methodology for the preliminary assessment of large space structures for various applications. The tetrahedral truss considered herein provides a baseline design against which other structural arrangements can be compared. It is estimated, however, for applications that require the open truss structure to be covered with a surface, the mass of the surface coverings could be as great or greater than the mass of the truss. A logical extension of the present work, therefore, is to include the mass and stiffness of the coverings so that a proper evaluation of such cases could be made.

## APPENDIX A

## MASS OF TUBULAR COLUMNS

In this appendix the masses of aluminum and graphite/epoxy tubular columns required to carry a given compressive load are presented. Reduction factors are applied to the local buckling and Euler buckling loads and minimum gage wall thicknesses are taken into account.

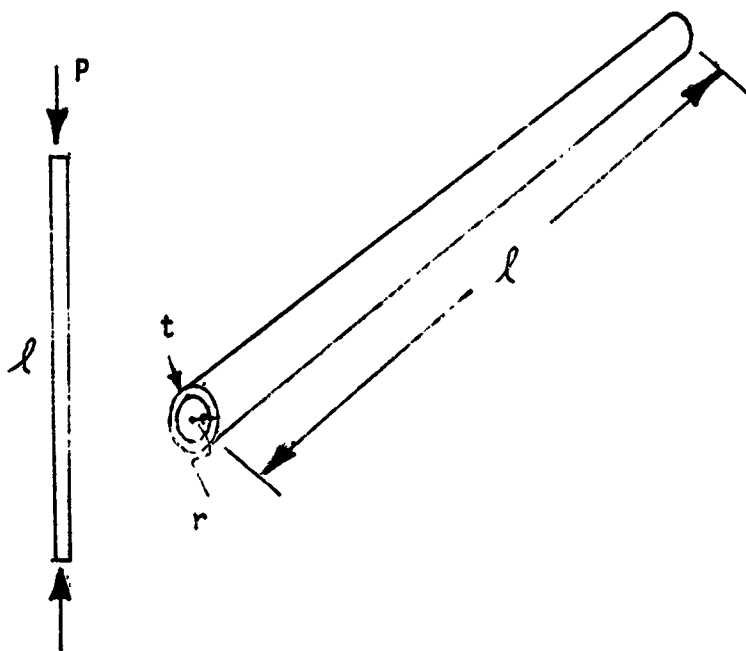
## Aluminum Columns

A schematic of the column considered and pertinent dimensions are shown in sketch A-a.

$$A_c = 2\pi r t$$

$$I_c = \pi r^3 t$$

$$W_c = \rho_c A_c l$$



Sketch A-a.- Column details

The column has a cross sectional area  $A_c$ , a moment of inertia  $I_c$ , a mass  $W_c$  and is loaded with a compressive load  $P$ . The Euler buckling load for a column is

$$P_{\text{Euler}} = \frac{c\pi^2 EI}{l^2} \quad (\text{A-1})$$

and the corresponding stress is

$$\sigma_{\text{Euler}} = \frac{P_{\text{Euler}}}{A_c} = \frac{c\pi^2 E r^2}{2l^2} \quad (\text{A-2})$$

where  $c$  is 1 for a perfect column pinned at both ends. The local wall buckling stress for a thin walled cylinder is

$$\sigma_{\text{local}} = c_1 \frac{Et}{r} \quad (\text{A-3})$$

where  $c_1$  is 0.6 for a perfect cylinder. The stress due to the applied compressive load is

$$\sigma_{\text{App.}} = \frac{P}{2\pi r t} \quad (\text{A-4})$$

Buckling Critical Columns.- For a minimum-weight column it is assumed that the stresses from equations (A-2), (A-3), and (A-4) are all equal. By eliminating  $r$  and  $t$  an expression for the buckling stress  $\sigma_b$  can be

obtained as follows:---

$$\sigma_{\text{Euler}} \sigma_{\text{local}} \sigma_{\text{App.}} = \sigma_b^3 = \frac{cc_1 \pi E^2 P}{4 \ell^2} \quad (\text{A-5})$$

Now considering that  $\sigma_b = P/A_c$  and  $A_c = \frac{W_c}{\rho_c \ell}$  an expression for the mass of a column  $W_c$  can be found from equation (A-5) as

$$W_c = \left( \frac{4}{cc_1 \pi} \right)^{1/3} \frac{\rho_c}{E^{2/3}} P^{2/3} \ell^{5/3} \quad (\text{A-6})$$

By dividing both sides of equation (A-6) by  $\ell^3$  the structural index form for the mass of a column is obtained as

$$\frac{W_c}{\ell^3} = \left( \frac{4}{cc_1 \pi} \right)^{1/3} \frac{\rho_c}{E^{2/3}} \left( \frac{P}{\ell^2} \right)^{2/3} \quad (\text{A-7})$$

mass
shape
material
loading  
parameter
factor
parameter
index

This form of the equation permits the mass parameter to be plotted as a function of the loading index independent of tube dimensions.

Minimum Gage Thickness Constrained Columns.- For small values of the compressive loading,  $P$ , the thickness of material required to carry the load becomes very small and in fact can be less than the practical minimum gage for the material being used. For this case, local buckling is no longer an active constraint and only Euler buckling need be considered. By eliminating  $r$  an expression for the buckling stress can be obtained as follows:

$$\sigma_{\text{Euler}} \sigma_{\text{App.}}^2 = (\sigma_b)_{\text{min.gage}}^3 = \frac{CEp^2}{8\ell^2 t^2} \quad (\text{A-8})$$

Proceeding as was done in obtaining equation (A-6) an expression for the mass of a column with a minimum gage thickness constraint  $t_m$  is found as.

$$(W_c)_{\text{min.gage}} = \left(\frac{8}{c}\right)^{1/3} \frac{\rho_c}{E^{1/3}} t_m^{2/3} p^{1/3} \ell^{5/3} \quad (\text{A-9})$$

In a structural index form similar to equation (A-7), the above equation becomes

$$\left(\frac{W_c}{\ell^3}\right)_{\text{min.gage}} = \left(\frac{8}{c}\right)^{1/3} \frac{\rho_c}{E^{1/3}} \left(\frac{t_m}{\ell}\right)^{2/3} \left(\frac{p}{\ell^2}\right)^{1/3} \quad (\text{A-10})$$

For this case with the minimum gage thickness constraint the mass parameter depends on the thickness to length ratio  $t/\ell$  as well as on the loading index.

Results and Discussion.- In this section numerical results are presented for aluminum tubes to demonstrate the application of the previously developed equations. The constants used in this study are as follows:

$$E_c = 68.9 \text{ GN/m}^2 \quad (10 \times 10^6 \text{ psi}) \quad (\text{A-11})$$

$$\rho_c = 2767 \text{ kg/m}^3 \quad (.1 \text{ lbm/in}^3)$$

$$c = .9, \quad c_1 = .36$$

The values of the buckling constants  $c$  and  $c_1$  are chosen to take account of buckling load reductions due to imperfections.

The masses of aluminum columns as determined from equations (A-7) and (A-10) for the values given in equations (A-11) are plotted in structural index form in figure 10. The minimum gage thickness for aluminum was chosen as  $t_m = .381$  mm (.015 inches). The light lines are the governing minimum gage masses of lightly loaded columns for the lengths indicated on the figure. The heavy line is the mass of a column when the loads are high enough that the minimum thickness is exceeded.

The material strains corresponding to the masses and loads of figure 10 are presented in figure 11. The strain in aluminum corresponding to a yield stress of  $275.8$  MP<sub>a</sub> (40,000 psi) is .004. It can be seen that for most of the load range considered in figure 11 the strains are well below this value. In fact for very low loads the strains are two orders of magnitude lower than the material yield strain.

#### Graphite/Epoxy Columns

The graphite/epoxy columns considered in this section have the same overall dimensions as shown in sketch A-a. The tube wall, however, is composed of longitudinal ( $0^\circ$ ) plies with circumferentially ( $90^\circ$ ) wrapped plies on the inside and outside to improve local buckling and handling characteristics. As was the case with the aluminum columns, for lightly loaded graphite/epoxy columns local skin buckling is not a constraint so that only Euler buckling governs the design. The mass of such minimum gage designed graphite/epoxy columns is given by equation (A-9) where  $t_m$  is the total thickness of minimum gage wall laminate considered and  $E$  is the corresponding modulus in the longitudinal direction. For higher loading conditions where local buckling of the column wall must be considered the orthotropic nature of the wall properties precludes obtaining a simple closed form mass equation as was done previously for isotropic columns. In the present study the local wall buckling was treated using the standard orthotropic cylinder buckling analysis from reference 7 with the same knockdown factor as was used in a previous section for isotropic columns. The Euler buckling was treated as in the

previous section with the same knockdown factor. These buckling constraints along with minimum lamina thickness constraints were coded using a nonlinear mathematical programming minimization technique such as in reference 8 to obtain minimum mass column proportions for the heavily loaded range.

Results and Discussion.- Results for the mass of graphite/epoxy columns as obtained from the approach discussed in the previous section are presented in structural index form in figure 12.

The lamina material properties and minimum thicknesses used in this study are as follows.

$$E_{11} = 131 \text{ GN/m}^2 (19.0 \times 10^6 \text{ lbf/in}^2)$$

$$E_{22} = 10.9 \text{ GN/m}^2 (1.58 \times 10^6 \text{ lbf/in}^2)$$

$$G_{12} = 6.41 \text{ GN/m}^2 (0.93 \times 10^6 \text{ lbf/in}^2)$$

$$\nu_{12} = 0.32$$

$$\rho_c = 1522 \text{ KG/m}^3 (0.055 \text{ lbf/in}^3)$$

$$t_{0^\circ} > .42 \text{ mm (.0165 in)}$$

$$t_{90^\circ} > .076 \text{ mm (.003 in)}$$

$$t_m > .57 \text{ mm (.0225 in)}$$

As was the case for the aluminum columns the light lines represent lightly loaded minimum gage thickness designs while the heavier lines represent heavily loaded designs constrained by local wall buckling. The smooth transition between the minimum gage thickness and the heavily loaded portions of the curve is due to the fact that the thicknesses of the  $0^\circ$  plies and the  $90^\circ$  plies are permitted to vary independently. Comparison of figures 10 and 12 indicates that in the lightly loaded portion the graphite/epoxy columns are about 40% less in mass than the corresponding aluminum columns for the minimum gage thicknesses used. The strains in the graphite/epoxy columns corresponding to the masses and loads of figure 12 are presented in figure 13.

Comparison of the strains at comparable load levels from figure 13 and from 11 shows that minimum mass graphite/epoxy columns are twice as stiff as minimum mass aluminum columns in the local buckling critical range and are 60% stiffer than minimum mass aluminum columns in the minimum gage thickness range.

## REFERENCES

1. NASA Task Group: Outlook for Space. NASA SP-386, January 1976.
2. Hedgepeth, John M.: Survey of Future Requirements for Large Space Structures. NASA CR-2621, 1975.
3. Davies, R. M., Editor: Space Structures. Blackwell Scientific Publications, 1967.
4. Bush, Harold G.; and Mikulas, Martin M., Jr.: A Nestable, Tapered Column Concept For Large Space Structures. NASA TM X-73927, 1976.
5. Ashton, J. E.; Halpin, J. C.; and Petit, P. H.: Primer on Composite Materials: Analysis. Technomic Publishing Co., Inc., 1969.
6. Timoshenko, S.: Vibration Problems in Engineering. D. Van Nostrand Co., Inc., N.Y., May 1947.
7. Block, David L.; Card, Michael F.; and Mikulas, Martin M., Jr.: Buckling of Eccentrically Stiffened Orthotropic Cylinders. NASA TN D-2960, August 1965.
8. Stroud, W. Jefferson; and Agranoff, Nancy: Minimum-Mass Design of Filamentary Composite Panels Under Combined Loads: Design Procedure Based on Simplified Buckling Equations. NASA TN D-8257, October 1976.

ORIGINAL PAGE IS  
OF POOR QUALITY

PRECEDING PAGE BLANK NOT FILMED

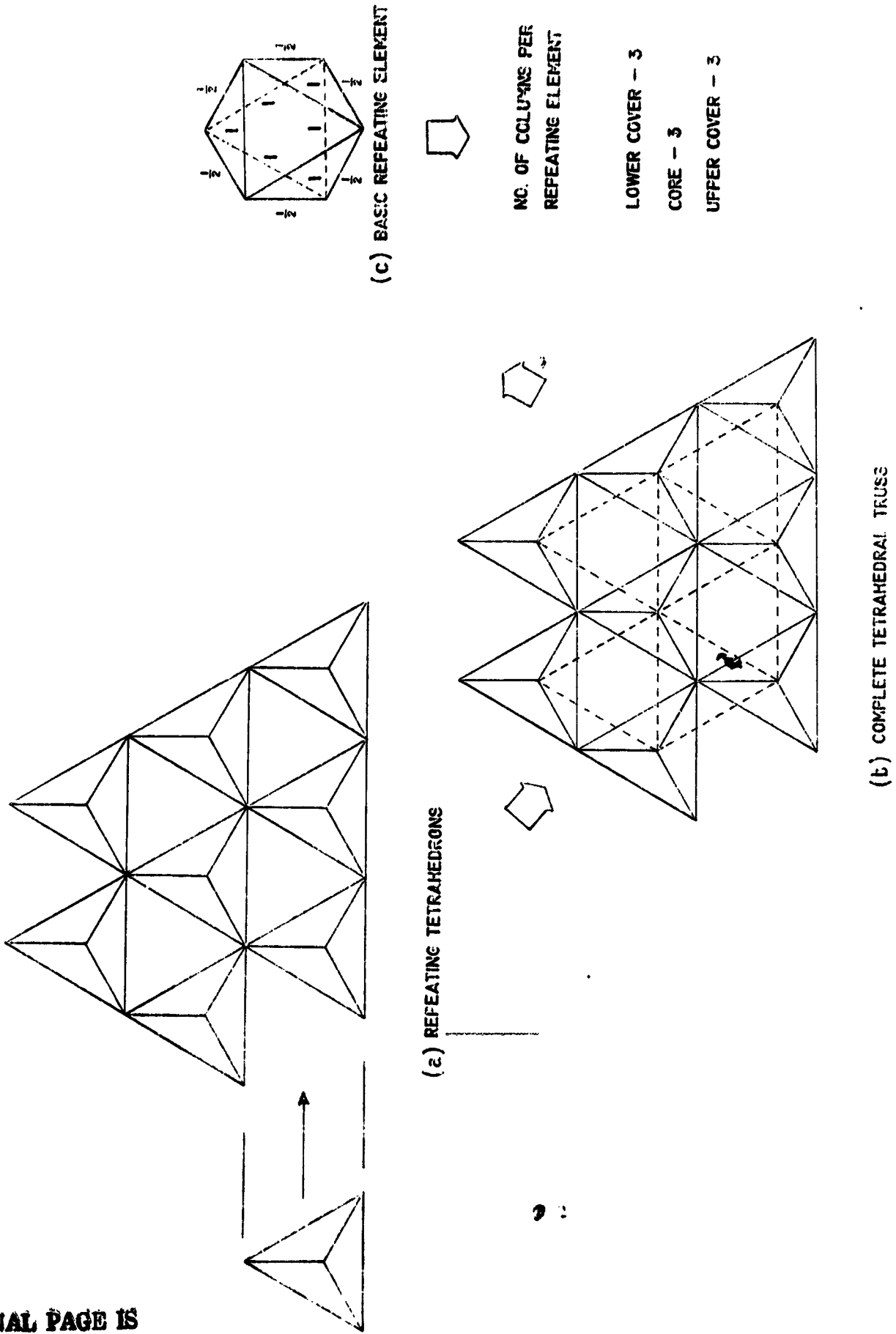


Figure 1. Tetrahedral truss construction.

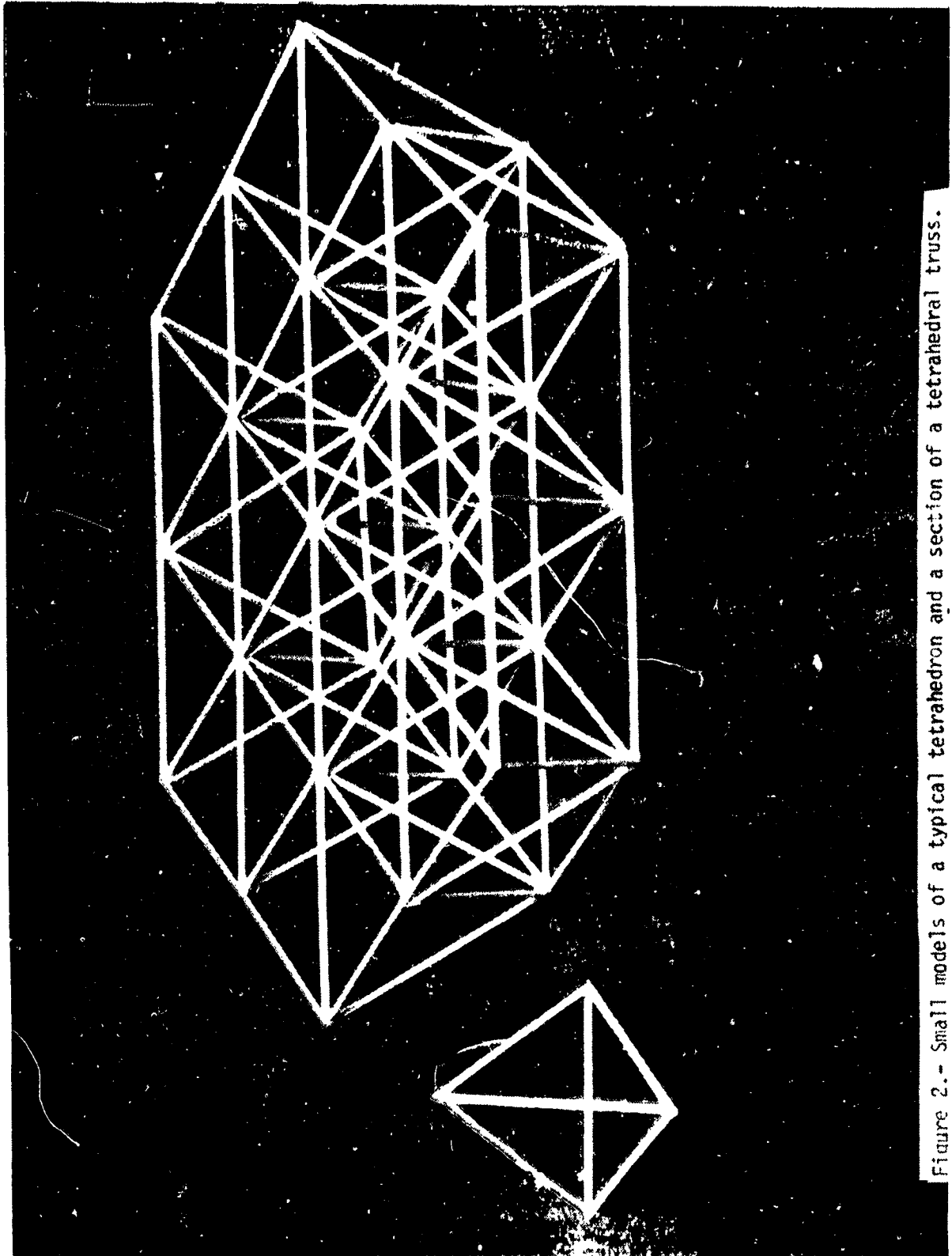


Figure 2.- Small models of a typical tetrahedron and a section of a tetrahedral truss.

ORIGINAL PAGE IS  
OF POOR QUALITY

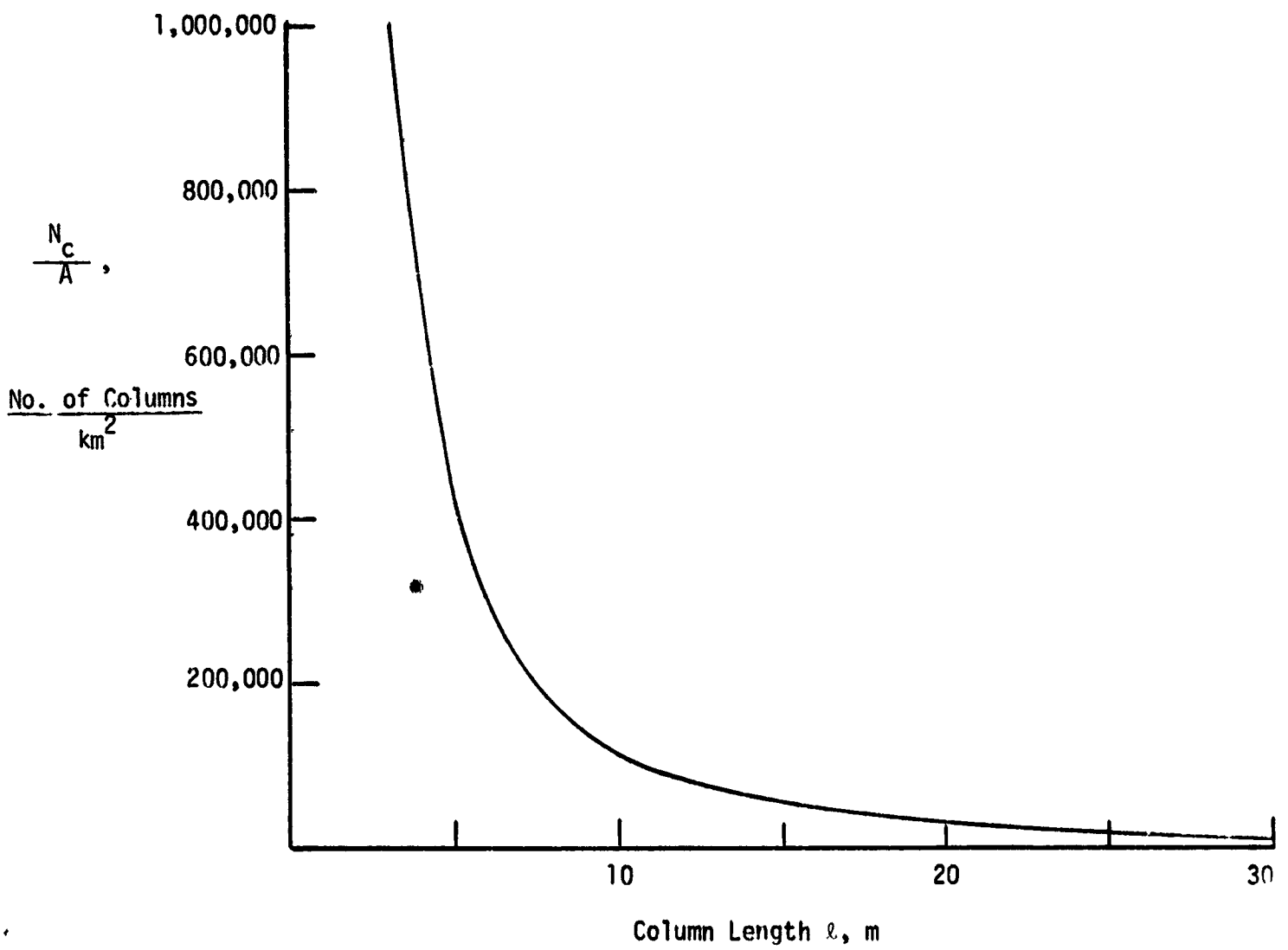


Figure 3.- Number of columns per square kilometer in a tetrahedral truss as a function of column length.

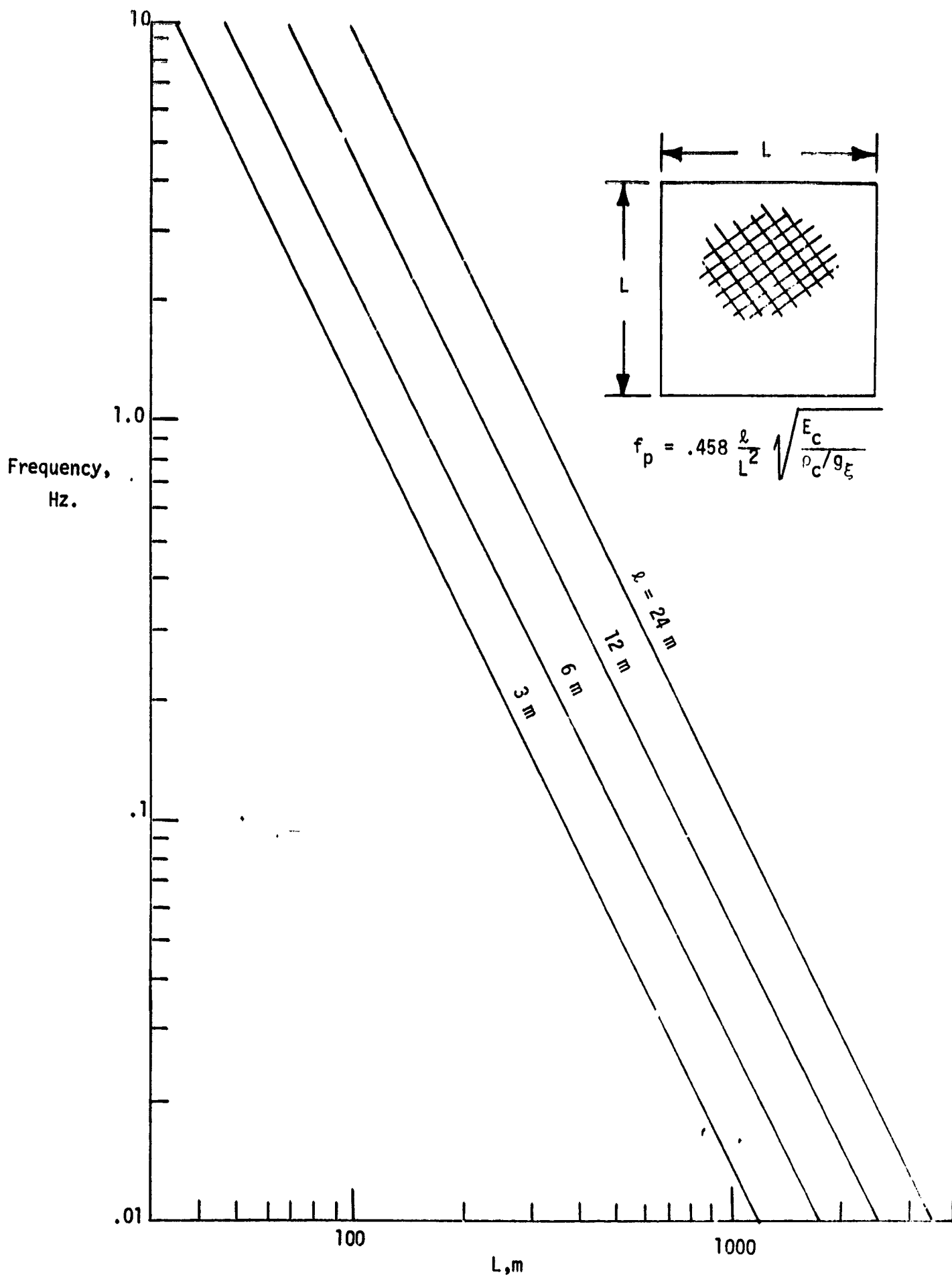


Figure 4. First natural frequency of a free-free isotropic plate with a grid.

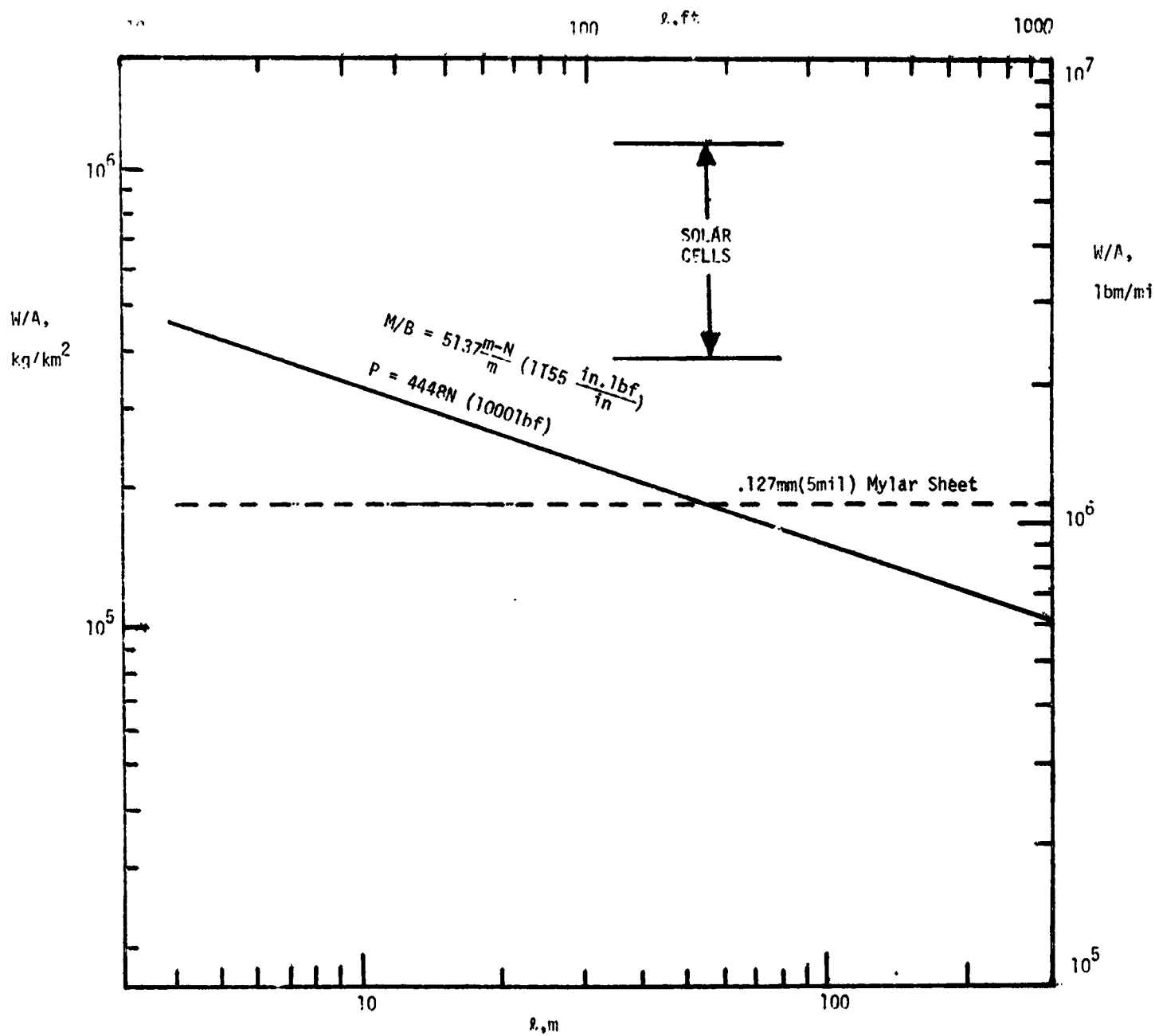


Figure 5.- Truss mass per unit area required to carry an applied moment.

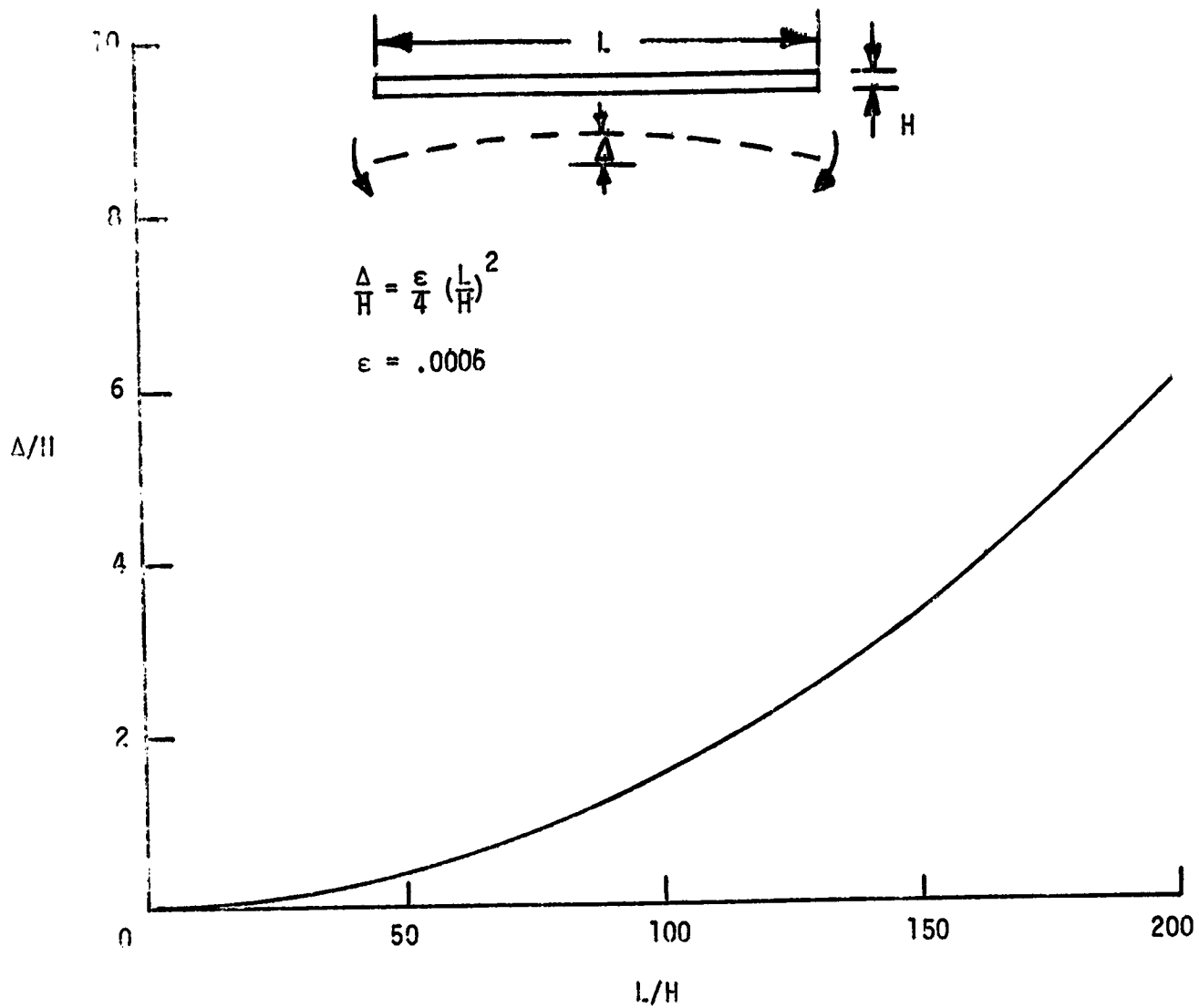


Figure 6.- Lateral displacement of a tetrahedral truss structure subjected to a pure bending moment.

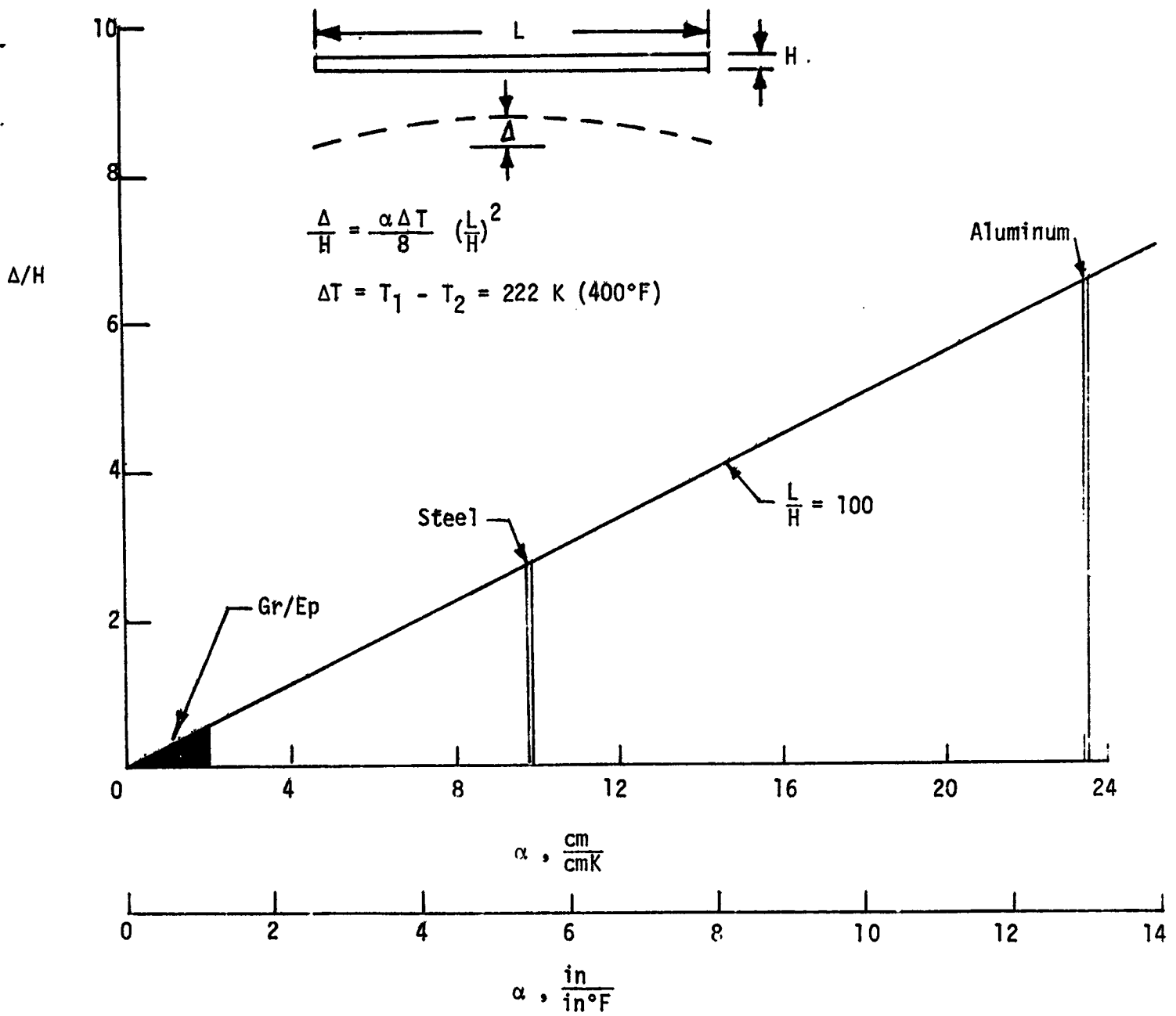


Figure 7.- Lateral displacement of a tetrahedral truss structure subjected to a temperature differential  $\Delta T$  across the truss depth.

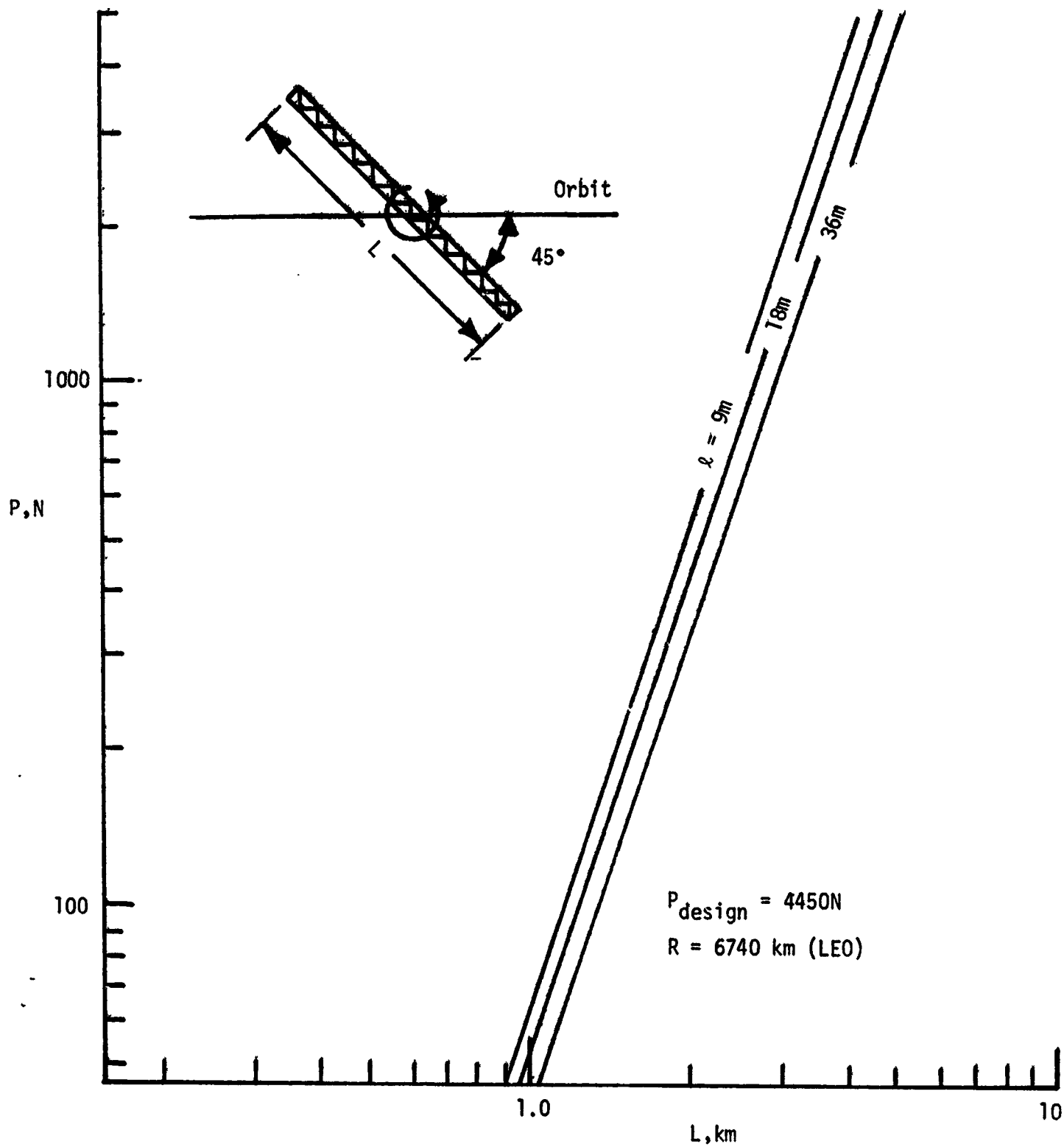


Figure 8.- Maximum load in columns due to gravity gradient restoring moment.

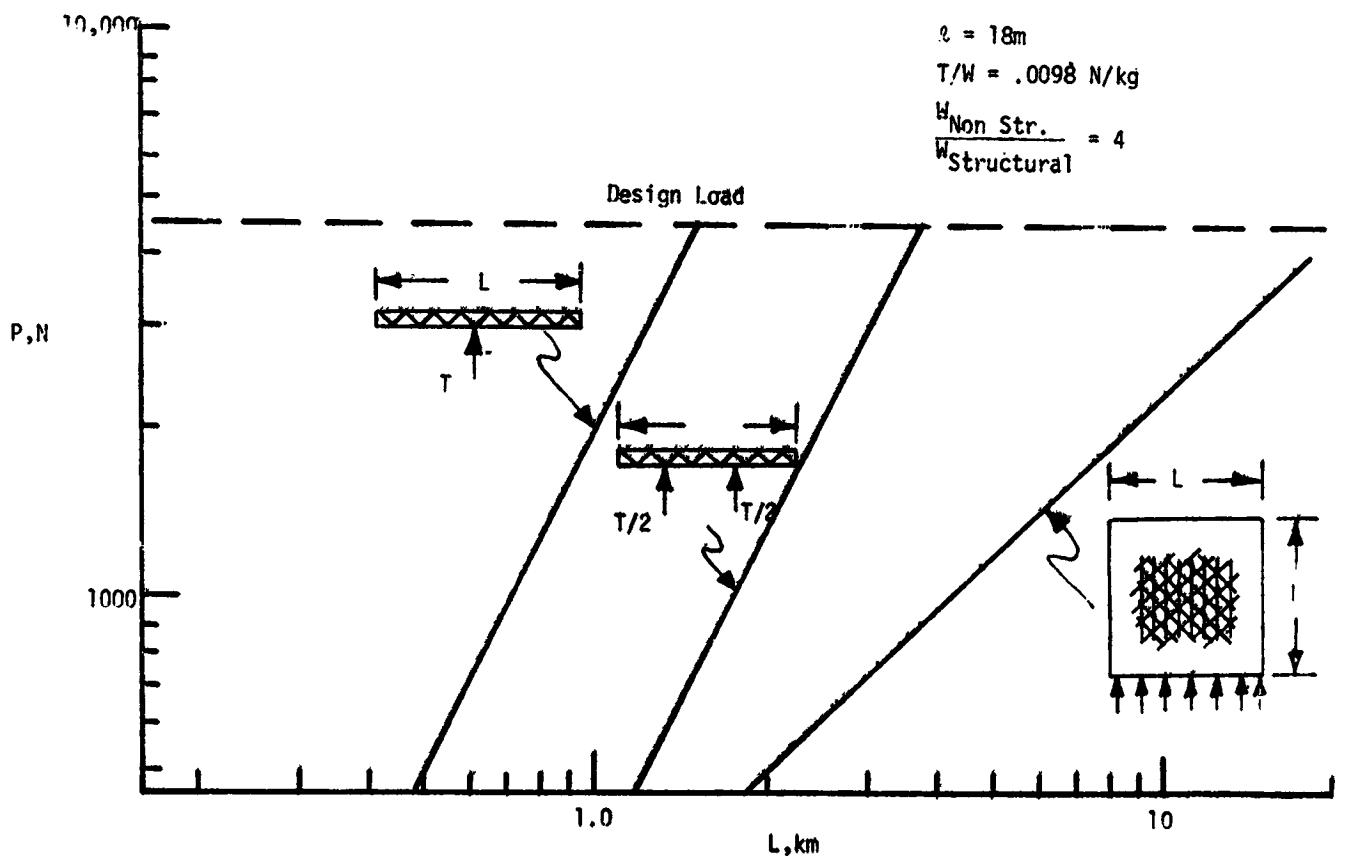


Figure 9.- Column load due to orbital transfer thrust loading.

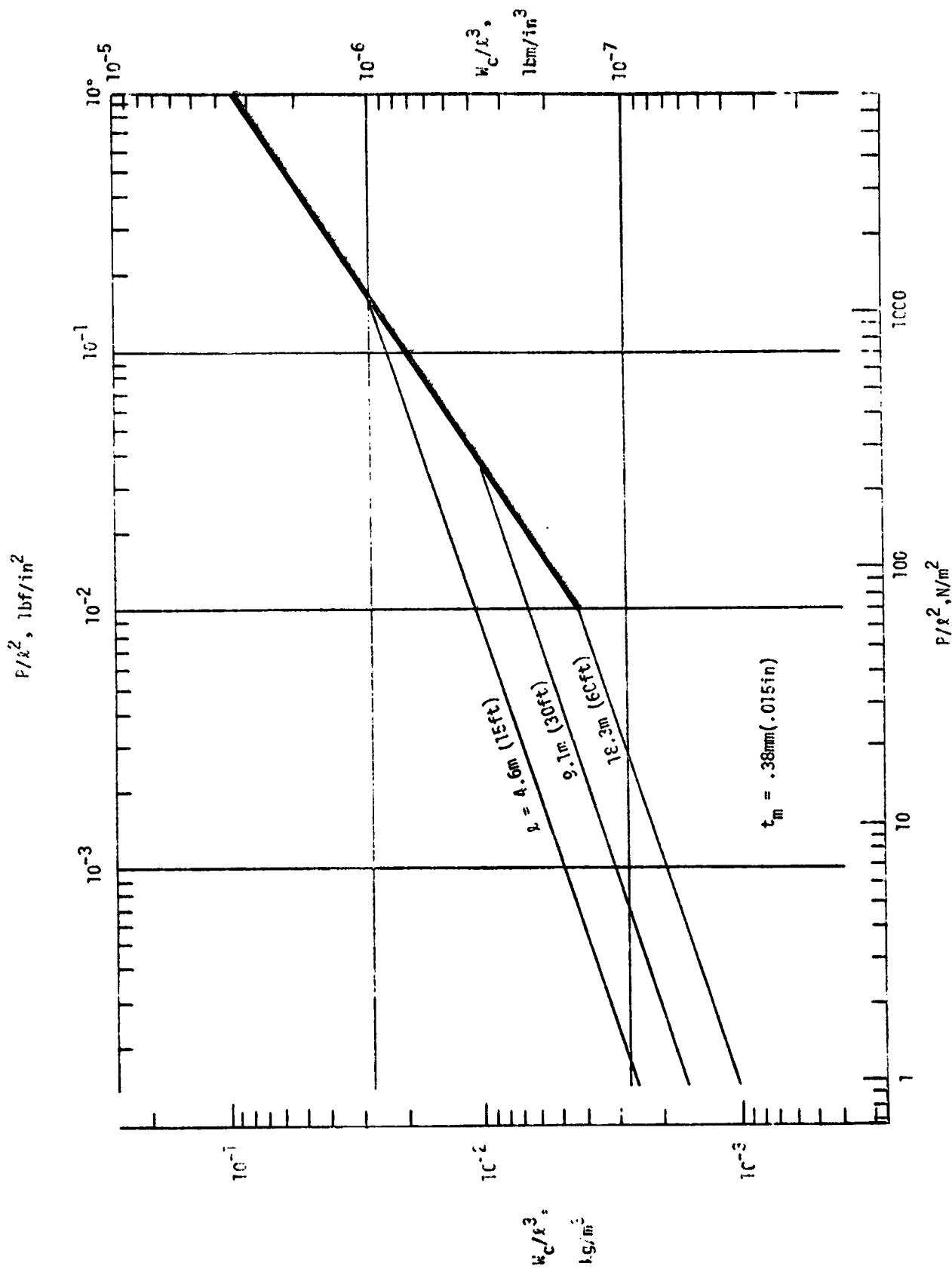


Figure 10.- Weight of thin-walled tubular aluminum columns.

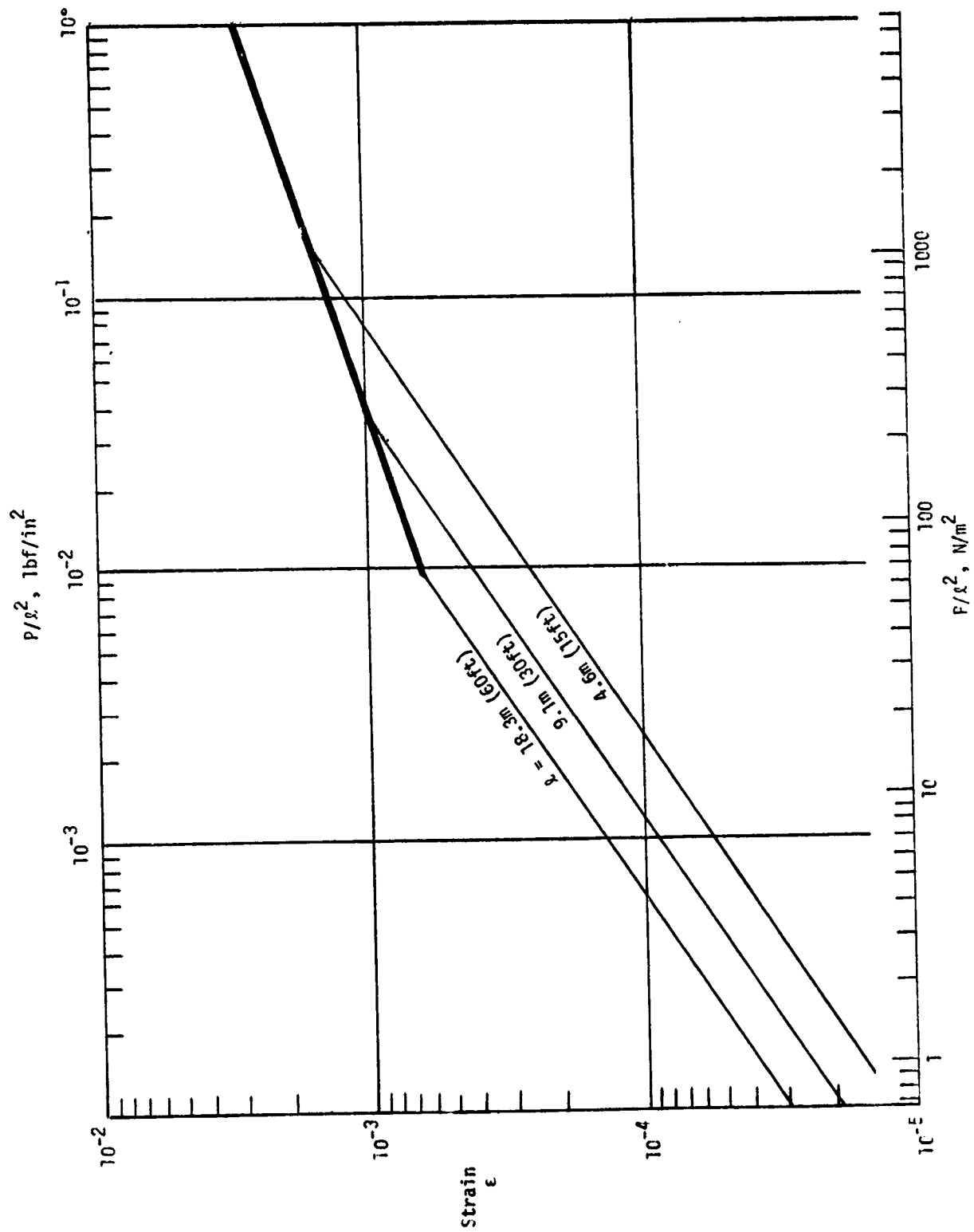


Figure 11.- Axial strain at buckling in a thin-walled aluminum column.

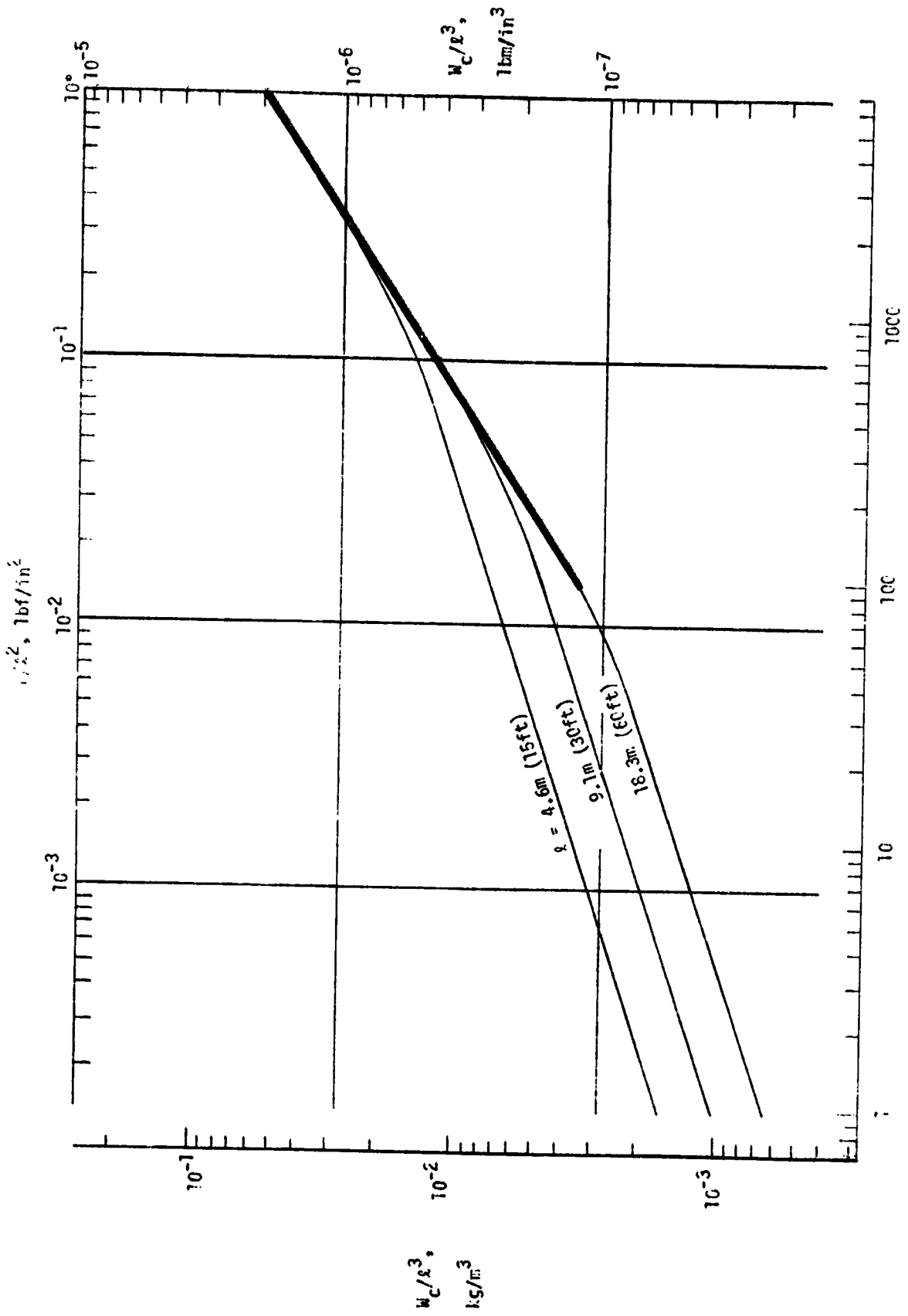


Figure 12.- Weight of thin-walled tubular graphite/epoxy columns.

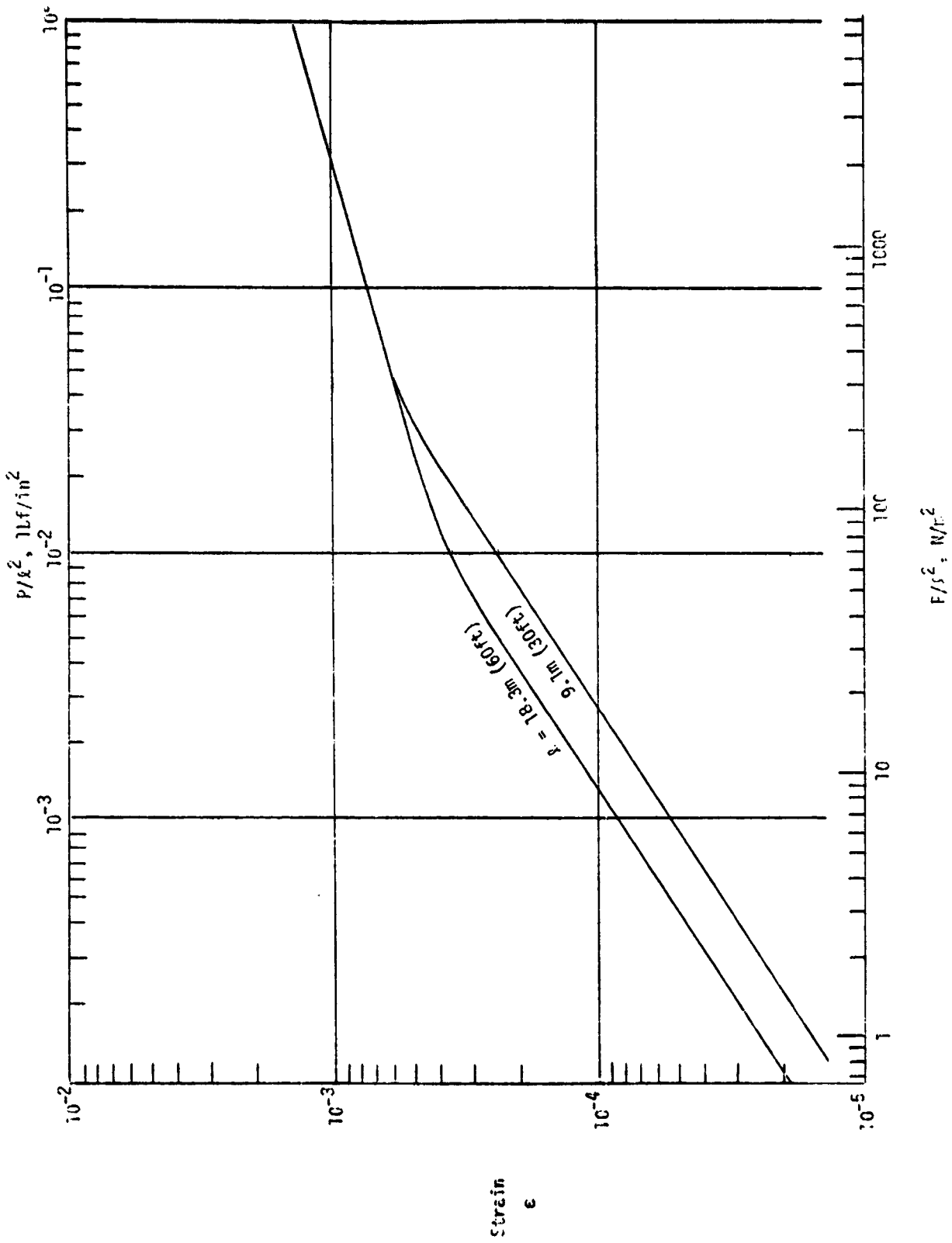


Figure 15. Axial strain at buckling in a thin-walled graphite/epoxy column.